

# Acute and Chronic Shear Stress Differently Regulate Endothelial Internalization of Nanocarriers Targeted to Platelet-Endothelial Cell Adhesion Molecule-1

Jingyan Han,<sup>†</sup> Blaine J. Zern,<sup>†</sup> Vladimir V. Shuvaev,<sup>†</sup> Peter F. Davies,<sup>‡</sup> Silvia Muro,<sup>§</sup> and Vladimir Muzykantov<sup>\*,†</sup>

<sup>†</sup>Department of Pharmacology and Center for Translational Targeted Therapeutics and Nanomedicine of the Institute for Translational Medicine and Therapeutics, and <sup>‡</sup>Department of Pathology and Institute for Medicine and Engineering, Perelman School of Medicine, University of Pennsylvania, Philadelphia, Pennsylvania 19104, United States, and <sup>§</sup>Fischell Department of Bioengineering, University of Maryland, College Park, Maryland 20742, United States

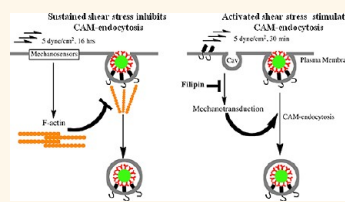
Numerous advanced drug delivery systems using nanocarriers (NC) are being currently designed and tested to optimize the cellular location, amplitude, and timing of desirable effects of drugs. It is well appreciated that parameters of carrier design (e.g., geometry, size, plasticity, controlled disassembly, valence, affinity to anchoring epitopes, and ability to interact with cell membranes) play an important role in cellular entry and subsequent intracellular itinerary of the carrier and cargo.<sup>1–4</sup> On the other hand, specific features of the target cell phenotype and its functional status, controlled by systemic and microenvironment factors, undoubtedly modulate intracellular delivery; yet this aspect of the problem is often overlooked. The majority of studies of intracellular delivery of nanocarriers employ generic cellular models having insufficient resemblance to local target cell conditions and behavior *in vivo*.<sup>1–8</sup> This shortcoming necessitates the use of models more adequately reflecting phenotypic features of target cells.

Endothelial cells (EC) lining the luminal surface of blood vessels represent an important and specific target for biomedical interventions. To optimize delivery, drugs can be targeted to the endothelium using ligand binding to the endothelial surface molecules.<sup>9</sup> In particular, the endothelial glycoproteins platelet-endothelial cell adhesion molecule-1 (PECAM) and intercellular adhesion molecule-1 (ICAM) are useful targets for endothelial drug delivery.<sup>10</sup> Following intravascular injection in animal models, drugs conjugated with ligands of these cell adhesion molecules (CAMs) bind to endothelium

**ABSTRACT** Intracellular delivery of nanocarriers (NC) is controlled by their design and target cell phenotype, microenvironment, and functional status. Endothelial cells (EC) lining the vascular lumen represent an important target for drug delivery. Endothelium *in vivo* is

constantly or intermittently (as, for example, during ischemia-reperfusion) exposed to blood flow, which influences NC–EC interactions by changing NC transport properties, and by direct mechanical effects upon EC mechanisms involved in NC binding and uptake. EC do not internalize antibodies to marker glycoprotein PECAM(CD31), yet internalize multivalent NC coated with PECAM antibodies (anti-PECAM/NC) via a noncanonical endocytic pathway distantly related to macropinocytosis. Here we studied the effects of flow on EC uptake of anti-PECAM/NC spheres (~180 nm diameter). EC adaptation to chronic flow, manifested by cellular alignment with flow direction and formation of actin stress fibers, inhibited anti-PECAM/NC endocytosis consistent with lower rates of anti-PECAM/NC endocytosis *in vivo* in arterial compared to capillary vessels. Acute induction of actin stress fibers by thrombin also inhibited anti-PECAM/NC endocytosis, demonstrating that formation of actin stress fibers impedes EC endocytic machinery. In contrast, acute flow without stress fiber formation, stimulated anti-PECAM/NC endocytosis. Anti-PECAM/NC endocytosis did not correlate with the number of cell-bound particles under flow or static conditions. PECAM cytosolic tail deletion and disruption of cholesterol-rich plasmalemma domains abrogated anti-PECAM/NC endocytosis stimulation by acute flow, suggesting complex regulation of a flow-sensitive endocytic pathway in EC. The studies demonstrate the importance of the local flow microenvironment for NC uptake by the endothelium and suggest that cell culture models of nanoparticle uptake should reflect the microenvironment and phenotype of the target cells.

**KEYWORDS:** intracellular delivery · endothelial cells · vascular immunotargeting · cell adhesion molecules · endocytosis · fluid shear stress



and exert therapeutic effects superior to those afforded by nontargeted drugs.<sup>11–14</sup> These encouraging results lead to the next level of complexity and sophistication, that is, control of the intracellular delivery of drug carriers targeted to endothelium.

PECAM and ICAM represent rather an unusual target for intracellular delivery. In

\* Address correspondence to muzykantov@mail.med.upenn.edu.

Received for review June 18, 2012 and accepted September 7, 2012.

Published online September 08, 2012  
10.1021/nn302687n

© 2012 American Chemical Society

a more conventional approach, researchers prefer for this purpose to anchor carriers to membrane molecules that constitutively undergo internalization.<sup>15–17</sup> In contrast, endothelial cells do not effectively internalize ICAM and PECAM antibodies. However, the multivalent binding of nanocarriers carrying multiple antibody copies (e.g., anti-PECAM/NC) triggers a non-canonical vesicular uptake pathway known as CAM-endocytosis.<sup>18,19</sup> This pathway, distinct from clathrin-mediated or caveolar endocytosis, phagocytosis and pinocytosis, has a utility for intraendothelial delivery of diverse carriers and cargoes including therapeutic enzymes.<sup>20–22</sup> Understanding of the factors modulating this pathway will help to further optimize the design and use of therapeutics targeted to the endothelium.

The distinct molecular mechanism of CAM-endocytosis involves (i) PECAM clustering by multivalent anti-PECAM/NC, which causes tyrosine phosphorylation in the PECAM cytoplasmic domain, providing an endocytosis signal(s) mediated by activation of sodium-proton exchanger-1 (NHE-1), protein kinase C (PKC), c-src, and RhoA; and (ii) the rapid formation of actin stress fibers that are essential for CAM-endocytosis.<sup>19,23</sup>

Previous studies of anti-PECAM/NC endocytosis have employed endothelial cells *in vitro* in the absence of flow. However, except for physiologically underperfused or pathologically ischemic vascular regions, endothelium *in vivo* is exposed to hemodynamic forces imposed by blood flow. Blood is a heterogeneous suspension of circulating cells that exhibits complex dynamic characteristics at different flow velocities and other variable parameters including pulsatile *versus* steady flow (as in arteries *vs* in many other segments of the vasculature), wall geometries, and vessel calibers. Hemodynamic factors exert a powerful influence on the local functional phenotype of the endothelium.<sup>24,25</sup> A prominent feature of endothelial adaptation to flow is the formation of actin stress fibers and cell alignment with direction of flow.<sup>26</sup> Under flow, carriers possessing affinity to endothelial cell adhesion molecules behave similarly to leukocytes, that is, roll over and subsequently adhere to endothelium.<sup>27–29</sup> In addition, studies of the uptake of natural ligands including lipoproteins suggest that flow-driven movement of carriers adhering to endothelium can modulate endocytic signaling.<sup>30–33</sup> Therefore, the uptake of anti-PECAM/NC may be affected by both flow conditions and the cellular reactions to flow.

The role of flow in endothelial delivery of nanocarriers, especially their anchoring to the cells, has recently attracted considerable attention.<sup>28,34–36</sup> The flow characteristics, which vary considerably in different vascular beds and locations, greatly influence the NC availability to and anchoring on the endothelial surface. The transport of carriers into the boundary layer of the endothelial surface is a function of the local hemodynamics, and once the carrier is anchored,

torque and drag forces act upon the particles and the endothelial surface (wall shear stress).<sup>37</sup> Furthermore, carrier attachment and uptake are influenced by the size, shape, avidity, and valence of the particles and the functional status of the endothelium (e.g., density of target epitopes on the endothelial cell surface).<sup>38–40</sup> However, nothing is known about the effects of flow on endothelial endocytosis of nanocarriers targeted to PECAM, a stably expressed pan-endothelial cell adhesion molecule implicated in sensing of shear stress.<sup>41</sup> Here we report the distinct effects of acute and chronic flow and its associated shear stresses on endocytosis of anti-PECAM/NC by the endothelium.

## RESULTS AND DISCUSSION

**Anti-PECAM/NCs Endocytosis in the Pulmonary Vasculature of Mice.** To first establish physiological relevance, we studied endothelial endocytosis of anti-PECAM/NC *in vivo*. FITC-labeled (green) spherical polystyrene particles coated with ~200 PECAM antibody molecules per particle with final size ~180 nm in diameter (indicated thereafter as Ab/NC, unless indicated otherwise) were intravenously injected in mice. A total of 30 min later, pulmonary vasculature was perfused to wash out unbound materials and to identify surface-accessible particles by the infused fluorescently labeled red-secondary antibody, yielding double-label yellow color of particles on the luminal surface. Phase-contrast microscopy of lung tissue (left panel of Figure 1A) shows the longitudinal section of a blood vessel (~100  $\mu\text{m}$  in diameter) recognized as an arteriole in virtue of its thick muscular tunica media, size, and close proximity to bronchiole. Pulmonary capillaries (<10  $\mu\text{m}$  in diameter) wrap over the alveolar surfaces, forming an extremely thin blood–gas interface. The corresponding fluorescence image (right panel of Figure 1A) indicates that pulmonary uptake of anti-PECAM/NC was specific. Supporting Information, Figure 1 shows that level of fluorescent signal from the lung tissue obtained from mice 30 min after injection of control IgG/NC was negligible. This data square well with studies showing that pulmonary uptake of isotope-labeled anti-PECAM/NC after intravascular injection is an order of magnitude higher than that of IgG/NC.<sup>13,42,43</sup>

Of note, quantitative analysis of yellow (surface-bound) *versus* green (internalized) particles showed that the internalization level of Ab/NC in capillaries was higher than that in arterial vessels (Figure 1C). Hydrodynamic differences in these segments of vasculature may be responsible for differential uptake.

**Endothelial Endocytosis Is Related to the Avidity, But Not the Number of Cell-Bound Anti-PECAM/NC.** CAM-endocytosis is induced by cross-linking of anchoring molecules (e.g., PECAM) in the endothelial plasmalemma. The engagement of more PECAM copies by cell-bound particles may induce more potent endocytic signals. This can be achieved by (i) Ab/NC carrying more antibody

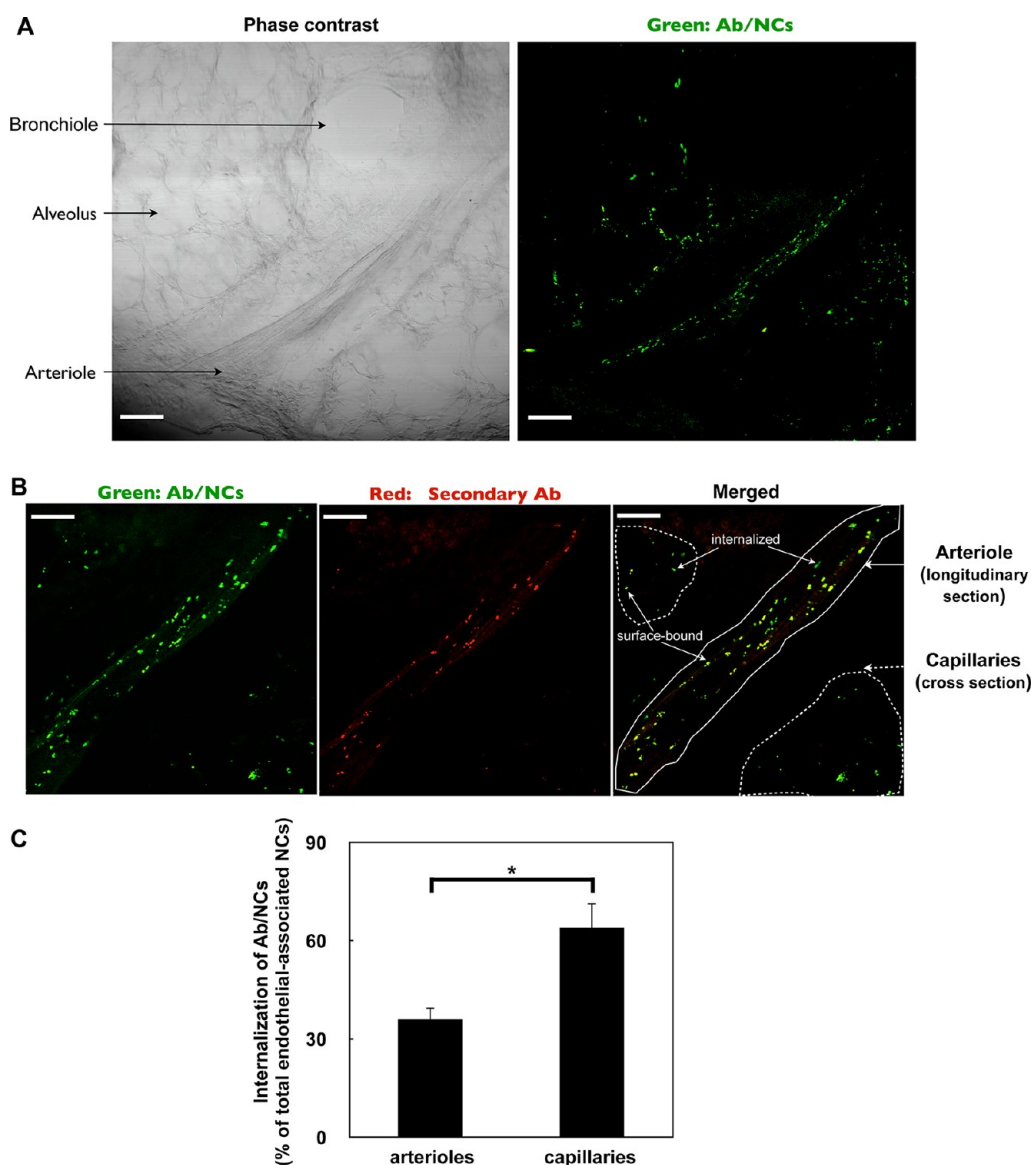


**Figure 1.** Endocytosis of anti-PECAM/NCs targeted to pulmonary vasculature *in vivo*. (A) Visualization of pulmonary uptake of green fluorescence-labeled anti-PECAM/NC *in vivo*. Phase contrast (left) and fluorescence (right) images of a tissue section of the lung obtained from a mouse 30 min after intravenous injection of anti-PECAM/NC (Ab/NC below). At post-mortem, lung was perfused through pulmonary artery with RPMI medium for 5 min to remove unbound intravascular materials prior to fixation and slicing. Scale bars, 100  $\mu\text{m}$ . (B) Endocytosis of Ab/NC in the pulmonary vasculature. A total of 30 min after intravenous injection of Ab/NC, lungs were perfused with buffer, as in panel A, and perfused further for 15 min with buffer containing Alexa Fluor 594 goat antirat IgG to counterstain surface-bound Ab/NC, followed by buffer perfusion to eliminate nonbound intravascular materials prior to fixation and slicing. Lung sections were analyzed with confocal fluorescence microscopy. Merged images show internalized Ab/NC as single-color labeled green particles and surface-bound Ab/NC as double-color labeled yellow particles. Scale bars, 40  $\mu\text{m}$ . (C) The internalization was expressed as percentage of total amount of endothelial-associated NCs internalized. Data were collected from 6 images for each group. Values are expressed as mean  $\pm$  SE ( $n = 6$ ),  $*p < 0.05$ .

molecules per particle (modulation of the strength of endocytic signal induced by individual particle); and (ii) binding more particles per cell (modulation of the strength of cumulative endocytic signaling). A recent computational study provides an example of the latter scenario ("cooperative endocytosis"), in which endocytosis increases proportionally to the dose of NC binding to cellular receptors.<sup>44</sup> Clarification of this is important for inquiries into the role of flow in endocytosis because binding of Ab/NC at a given antibody

surface density is influenced by incubation time, Ab/NC concentration, and hydrodynamic parameters. In particular, flow greatly modulates binding of Ab/NC to endothelial cells.<sup>45</sup> If the endocytosis depends on number of cell-bound Ab/NC, interrogation of the effect of flow on endocytosis would be confounded by effects of flow on binding.

To define this aspect without the confounding effects of flow on binding, we used static endothelial cell culture (*i.e.*, EC grown to confluence and incubated

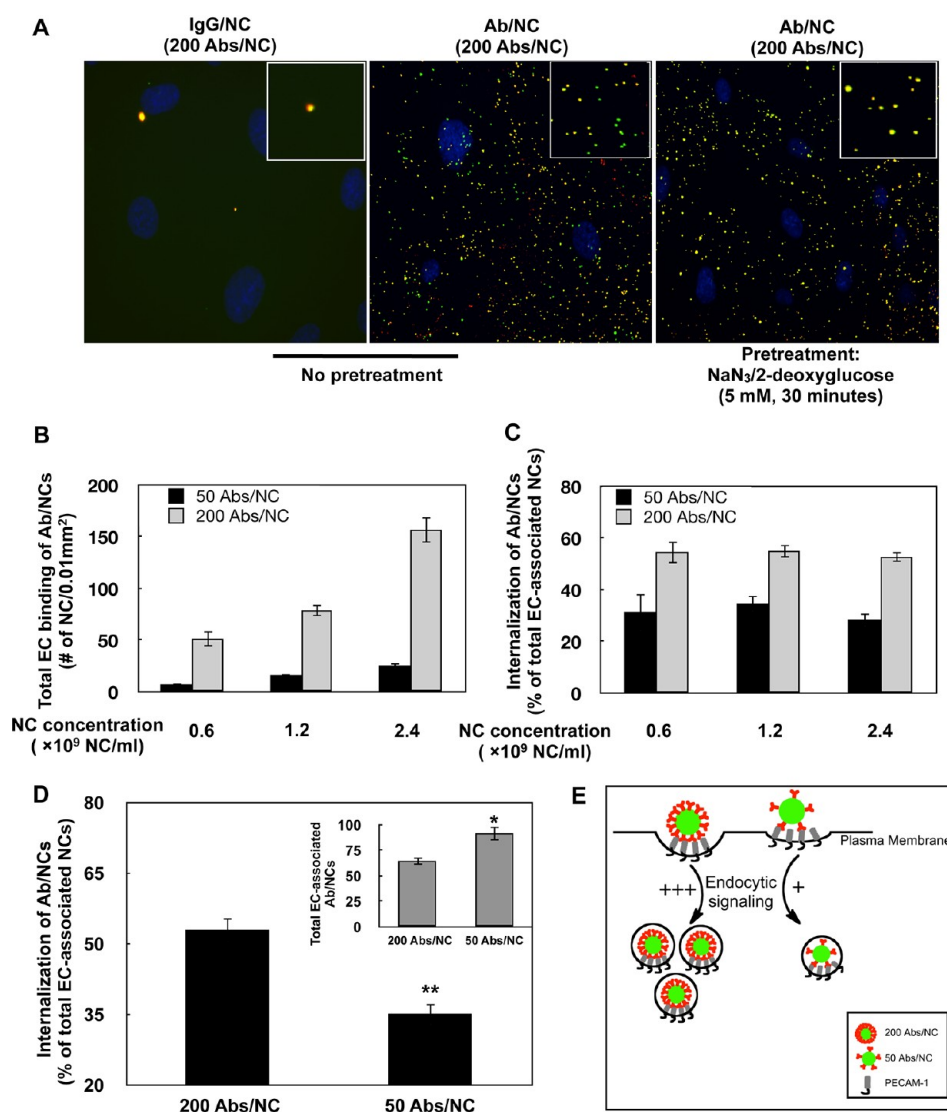


**Figure 2.** Endocytosis of anti-PECAM/NC in endothelial cell culture. (A) Static endothelial cells (EC) were incubated for 30 min at 37 °C with IgG/NC (left) of Ab/NC (middle and right), washed, and counterstained with secondary red anti-IgG. Merged fluorescence images show internalized (green) and surface-bound (yellow) Ab/NC in EC (middle). Endocytosis of Ab/NCs was blocked in ATP-depleted EC (right). (B) Endothelial binding (30 min incubation followed by washing) of Ab/NCs proportionally correlates with antibody surface density on particles and concentration of Ab/NC in incubation medium. Data were collected from eight images and presented as mean  $\pm$  SE ( $n = 8$ ). (C) Level of endocytosis of low and high avidity Ab/NC (50 and 200 Ab per particle) incubated with EC at indicated doses, as described in (B). (D) Internalization of low *versus* high avidity of Ab/NC incubated with EC at doses of 3 and  $1 \times 10^9$  NCs/mL, respectively, providing larger amount of cell-bound low-avidity Ab/NC *versus* high avidity Ab/NC (inset). In (C) and (D), the internalization was calculated as percentage of total amount of endothelial-bound Ab/NC, mean  $\pm$  SE ( $n = 8$ ); \* $p < 0.05$  and \*\* $p < 0.01$  in comparison with 200 Abs/NC group. (E) A schema represents the summary of results depicted in (B–D): endothelial endocytosis depends on the strength of the signal ignited by individual cell-bound Ab/NC (controlled by Ab surface density on a particle), not on the “collective” signaling by cell-bound Ab/NC (controlled by total number of cell-bound particles).

with Ab/NC in the absence of flow). Consistent with previous studies, Ab/NC, but not control IgG/NC, was bound and internalized by ECs *via* an active endocytosis that was blocked by inhibition of cellular metabolism (Figure 2A).

An elevation of either Ab/NC dose (*i.e.*, concentration of Ab/NC in the incubation medium) or Ab/NC avidity (attained by increase of the antibody surface density from 50 to 200 molecules per particle) enhanced binding (Figure 2B). Both factors proportionally modulated binding, that is, a 4-fold increase in either

Ab/NC dose or Ab surface density provided approximately 3-fold increase in number of Ab/NC bound per cell in the corresponding comparison group (compare black and gray bars at different doses in Figure 2B). As expected, the maximal binding was observed with high avidity Ab/NC at highest dose.

Regardless of the dose, Ab/NC with a given avidity displayed a similar level of endocytosis (Figure 2C), despite large differences in the number of Ab/NC bound per cell at different doses of Ab/NC (Figure 2B). At all doses of Ab/NC tested, endocytosis level was consistently

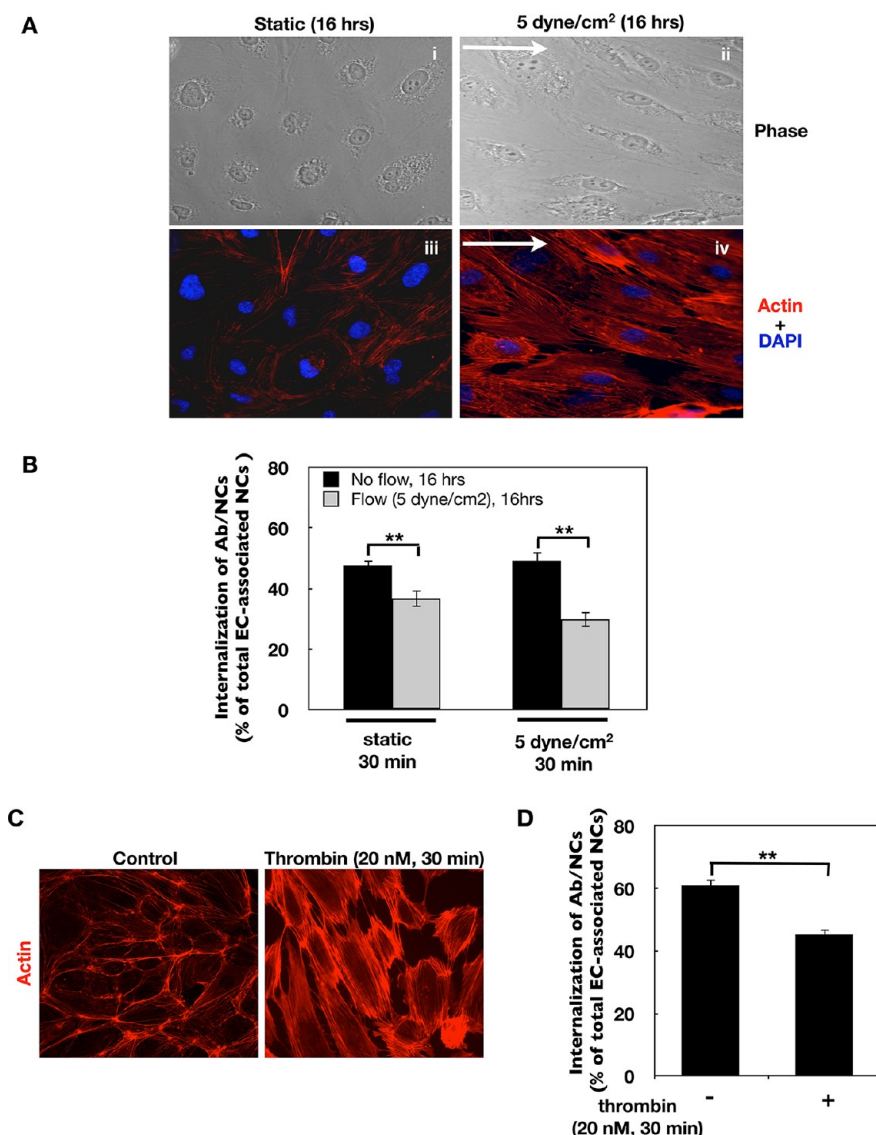


**Figure 3.** Endocytosis of anti-PECAM/NCs is inhibited in flow adapted EC. (A) Sustained exposure to flow induces EC alignment in the direction of flow and cytoskeletal remodeling. Confluent EC were exposed to static condition (i, iii) or 5 dyn/cm<sup>2</sup> laminar fluid shear stress (ii, iv) for 16 h. Cells were then fixed and stained for F-actin using Alexa-Fluor594-phalloidin. Images were taken using fluorescence microscope with a Plan Apo  $\times 40$  oil objective. Arrows show direction of flow. (B) In flow adapted EC, internalization of Ab/NC is inhibited. Cells were incubated or perfused (at 5 dyn/cm<sup>2</sup>) with HBSS medium containing anti-PECAM/NCs (200 Abs/NC,  $2 \times 10^9$  NCs/mL) for 30 min at 37 °C. Internalization was calculated and presented as mean  $\pm$  SE ( $n = 8$ ,  $**p < 0.01$ ). (C) Thrombin-induced cytoskeletal remodeling in EC. Confluent EC were incubated without or with thrombin (20 nM) for 30 min, followed by immunostaining for F-actin. (D) Internalization of Ab/NC is inhibited in thrombin-treated EC. Mean  $\pm$  SE ( $n = 8$ ,  $**p < 0.01$ ).

2-fold lower for low-avidity *versus* high-avidity Ab/NC:  $\sim 35$  *versus*  $\sim 55\%$ , respectively (Figure 2C). Figure 2D (and inset) demonstrates that the level of endocytosis of low-avidity Ab/NC was 2-fold lower than that of its high-avidity counterpart even at a high dose of low-avidity Ab/NC. Therefore, endothelial endocytosis of PECAM-bound Ab/NC is modulated by the strength of the signal induced by an individual particle anchored to the PECAM molecules, not the number of cell-bound Ab/NC (Figure 2E).

**Chronic Shear Stress and Acute Thrombin Challenge Inhibit Anti-PECAM/NC Endocytosis.** Endothelial cells in the arterial vasculature elongate during adaptation to high rates of

unidirectional laminar flow, whereas capillary endothelial cells exposed to low or oscillating flow assume a cobble-stone morphology similar to ECs in static cell culture.<sup>46,47</sup> To test the hypothesis that endocytosis of Ab/NC is less effective in arterial *versus* capillary endothelium (*cf.* Figure 1) due to structural changes associated with cell adaptation to flow, we tested the effects of chronic flow in EC.

Following a 16 h exposure to steady flow at 5 dyn/cm<sup>2</sup>, cells became elongated, oriented in the flow direction (Figure 3A, panels i and ii) and developed thick actin stress fibers (Figure 3A, panels iii and iv). Figure 3B shows that endocytosis of Ab/NCs was

diminished in the ECs adapted to flow for 16 h *versus* the ECs that had not been subjected to flow. This outcome was observed when flow-adapted EC were incubated with Ab/NC for 30 min in either static (Figure 3B, left bars) or flow (Figure 3B, right bars) conditions.

EC alignment and actin rearrangement represent two of many phenotype changes during adaptation to flow. To further probe the role of actin rearrangement in Ab/NC endocytosis, we tested whether rapid actin recruitment to the stress fibers, induced by a mechanism distinct from flow adaptation, would also affect endocytosis of Ab/NC. EC in static culture were incubated with thrombin just prior to adding Ab/NC. In accord with the literature, this led to fast (<30 min) actin reorganization into randomly oriented thick stress fibers (Figure 3C). Thrombin inhibited Ab/NC endocytosis to an extent similar to the effect of chronic shear stress (Figure 3D). PECAM, that serves in endothelial cells both as a cell–cell adhesion glycoprotein and signaling molecule, is involved in thrombin-induced endothelial gene expression (*e.g.*, tissue factor) and regulation of permeability.<sup>48,49</sup> However, the expression level and subcellular distribution of PECAM itself are not altered in thrombin-stimulated EC.<sup>48,49</sup> Consistent with these literatures, we found that thrombin caused no change in the binding of Ab/NC to EC ( $27.3 \pm 1.61$  vs  $26.6 \pm 1.07$  Ab/NC bound per cell), despite significant inhibition of endocytosis. This finding (i) affirms that Ab/NC endocytosis is a cellular reaction to the signal from an individual bound particle, rather than collective signal of cell-bound particles (see Figure 2), and (ii) suggests that the cytoskeleton rearrangements are involved in thrombin-induced inhibition of endothelial uptake of Ab/NC.

Taken together, the above data shows that (i) endocytosis of PECAM-targeted Ab/NC is less effective in arteries *versus* capillaries; (ii) chronic shear stress inhibits endocytosis of Ab/NC by endothelial cells; (iii) acute thrombin treatment has the same effect; and (iv) the inhibitory effects of chronic shear stress and acute thrombin exposure correlate with actin reorganization into stress fibers.

Interestingly, nanocarriers targeted to ICAM (anti-ICAM/NCs) also showed less effective endocytosis in arterial *versus* capillary endothelium *in vivo* and in flow-adapted *versus* static EC *in vitro*.<sup>50</sup> This similarity may be reflective of the fact that both ICAM and PECAM belong to the same Ig-superfamily of cell adhesion molecules and that endothelial cells employ CAM-endocytosis for uptake of both anti-PECAM/NC and anti-ICAM/NC. However, there are major differences between ICAM and PECAM. First, cytokine activation, which is necessary to up-regulate ICAM normally absent in cultured ECs, affects endocytosis.<sup>19,50,51</sup> Our recent study revealed that endotoxin challenge augments anti-ICAM/NC endocytosis *in vivo* in mouse

vasculature.<sup>50</sup> In contrast, PECAM is stably expressed by endothelium and the result observed in the present study is free of effects of cytokines. Next, ICAM and PECAM are localized in distinct domains of endothelial plasmalemma (lipid rafts *vs* intercellular borders), which may differentially affect flow modulation of Ab/NC endocytosis *via* these molecules. Furthermore, PECAM is known to be involved in flow-mediated signal transduction in endothelium, while such a role for ICAM has not been described.<sup>41,52</sup>

**Acute Shear Stress Stimulates Endothelial Endocytosis of Anti-PECAM/NCs.** To determine the effect of acute shear stress exposure during a period too short for endothelial adaptation to occur, ECs grown to confluence in the absence of flow were incubated for 30 min with Ab/NC under no-flow *versus* flow conditions. Such situations can be found *in vivo*, for example, in constitutively under-perfused vascular areas (such as blood vessels in the upper lung lobes) that become transiently perfused due to physiological mechanisms (*e.g.*, exertion), pathology (blood flow redistribution from hypoxic lobes), or medical interventions (*e.g.*, mechanical ventilation or cardio-pulmonary bypass).

To study the role of Ab/NC avidity and valency, we varied Ab density on the particle surface (50, 100, and 200 mAb molecules per particle). As expected, Ab/NC binding increased proportionally to Ab surface density under both static and flow conditions (Figure 4A). Acute flow stimulated the binding of high-avidity and suppressed binding of low-avidity Ab/NC (Figure 4A). Flow-mediated drag force and torque over particles adhering to ECs are expected to affect their binding in a manner dependent on particle avidity.<sup>35,45</sup> This helps to explain opposite effects of flow on binding of low *versus* high-avidity particles.

However, and opposite to the effect of chronic shear stress, acute flow stimulated the endocytosis of Ab/NCs in EC (Figure 4B). This effect was most prominent with low avidity Ab/NC (50 and 100 anti-PECAM per NC). Endocytosis of Ab/NC with lowest avidity was stimulated despite inhibition of binding. This finding provides additional support to the notion that Ab/NC endocytosis is related to the strength of the signal from an individual particle, not to the total number of cell-bound particles (*cf*: Figure 2).

Acute shear stress did not affect endocytosis of high-avidity Ab/NC (200 Abs/NC). Perhaps, particles carrying anti-PECAM at high surface density engage enough PECAM copies to achieve maximal endocytic signaling even in the absence of flow. Thus, low-avidity Ab/NC appears to be more sensitive probes for the defining modulation of endocytosis. Stimulation of endocytosis of low-avidity Ab/NC depended on the flow rate, which provided maximal effect at shear stresses in the range of 2–4 dyn/cm (Figure 4C).

In stimulation of endocytosis by acute increase in flow, rolling of anti-PECAM/NC on the endothelial

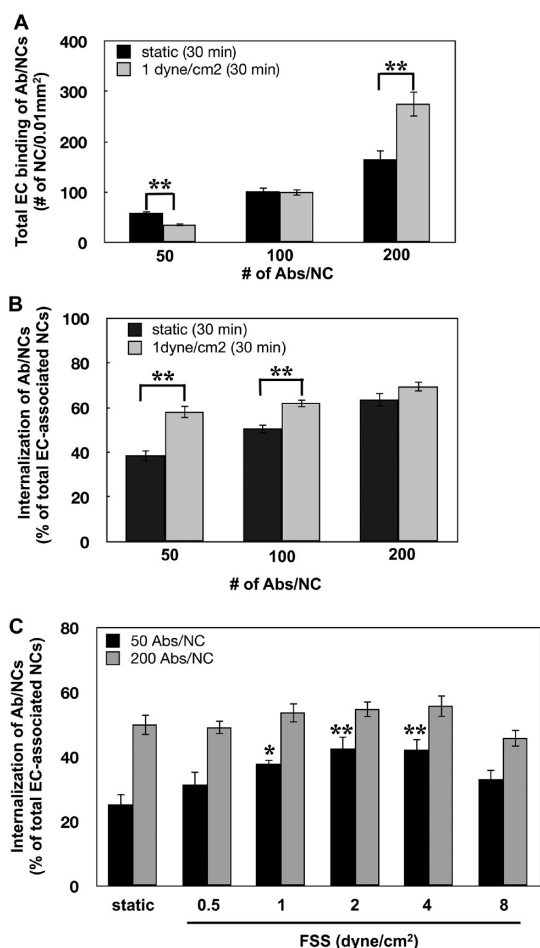


**Figure 4.** Acute exposure to flow stimulates endocytosis of anti-PECAM/NCS in EC. (A, B) Effect of flow (1 dyn/cm<sup>2</sup>, 30 min) on endothelial binding (A) and internalization (B) of Ab/NC carrying 50, 100, and 200 Ab molecules per NC. (C) Acute exposure to flow regulates endocytosis of Ab/NC (50 Abs/NC) in a flow rate-dependent manner. Data are presented as mean  $\pm$  SE ( $n = 8$ , \* $p < 0.05$ , \*\* $p < 0.01$ ).

surface may assist in engaging extra-copies of PECAM, thereby increasing the strength of endocytic signaling. Alternatively, torque force applied by flow on PECAM-anchored Ab/NC may cause stronger mechanical stimulation of the cell. Furthermore, acute increase in shear stress is known to cause many changes in the endothelial cells including elevation of cytosolic calcium, activation of NADPH-oxidase and other enzymatic pathways, some of which may interfere with endocytic machinery.<sup>53–55</sup> Therefore, there are many potential mechanisms for stimulation of Ab/NC endocytosis by acute shear stress.

**Signaling Involved in Stimulation of Endocytosis of Anti-PECAM/NC by Acute Flow.** Previously we found that signaling for Ab/NC endocytosis in static EC is mediated by tyrosine phosphorylation of PECAM cytosolic domain.<sup>23</sup> To test the role of this signaling pathway under acute flow, we studied endocytosis of high and low avidity Ab/NC using a model of endothelium-like monolayer of a mesothelioma REN cell line (null for

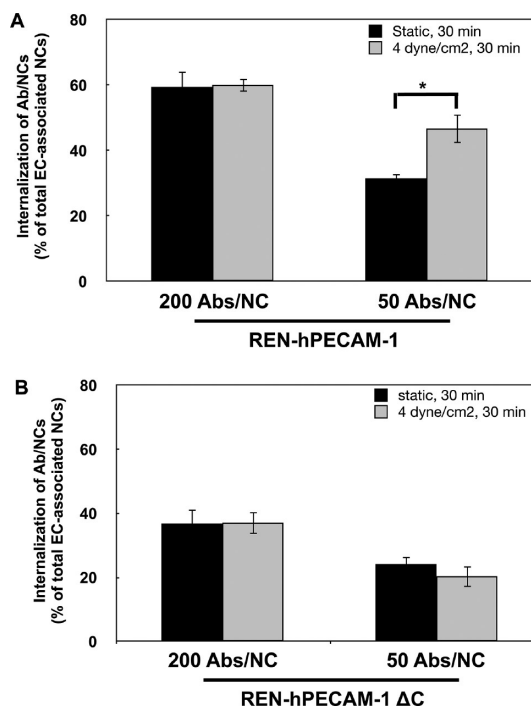


**Figure 5.** Cytoplasmic domain of PECAM-1 mediates stimulation of endocytosis of anti-PECAM/NCS by flow. (A) Flow stimulates endocytosis of low-avidity Ab/NC in REN cells stably transfected to express human PECAM-1. (B) Effect of flow-induced stimulation of endocytosis of Ab/NC is abolished in REN cells transfected with human PECAM-1 lacking the cytoplasmic domain. Data expressed as mean  $\pm$  SE ( $n = 6$ , \* $p < 0.05$ ).

PECAM) transfected with either full-length PECAM or PECAM with truncated cytosolic domain (REN/PECAM cells). Similar to what has been found in endothelial cells (Figure 4), acute flow stimulated endocytosis of low-avidity Ab/NC in REN/PECAM cells (Figure 5A). Furthermore, truncation of cytosolic PECAM domain abrogated this stimulatory effect (Figure 5B), indicating that acute shear stress stimulates the uptake of Ab/NC via CAM-endocytosis mediated by signals transduced by the PECAM cytosolic domain.

Unexpectedly, we also found that filipin, an agent disrupting cholesterol-rich domains in the plasma membrane, abrogated stimulation of endocytosis of low-avidity Ab/NC by acute flow (Figure 6A). In accord with previous results,<sup>19</sup> filipin had no effect on endocytosis of high-avidity Ab/NC under static conditions (Figure 6A), which supports low-avidity Ab/NC as a more sensitive probe for endocytic processes (Figures 4 and 5).

The unexpected inhibitory effect of filipin on stimulation of endocytosis of low-avidity Ab/NC by acute flow could be explained by several scenarios. Filipin-sensitive membrane domains including lipid rafts and caveoli exert the multifaceted endothelial functions including (i) transport from the milieu, providing openings into caveolar endosomes,<sup>16,56,57</sup> and (ii) mechano-sensing platforms in the plasmalemma mediating

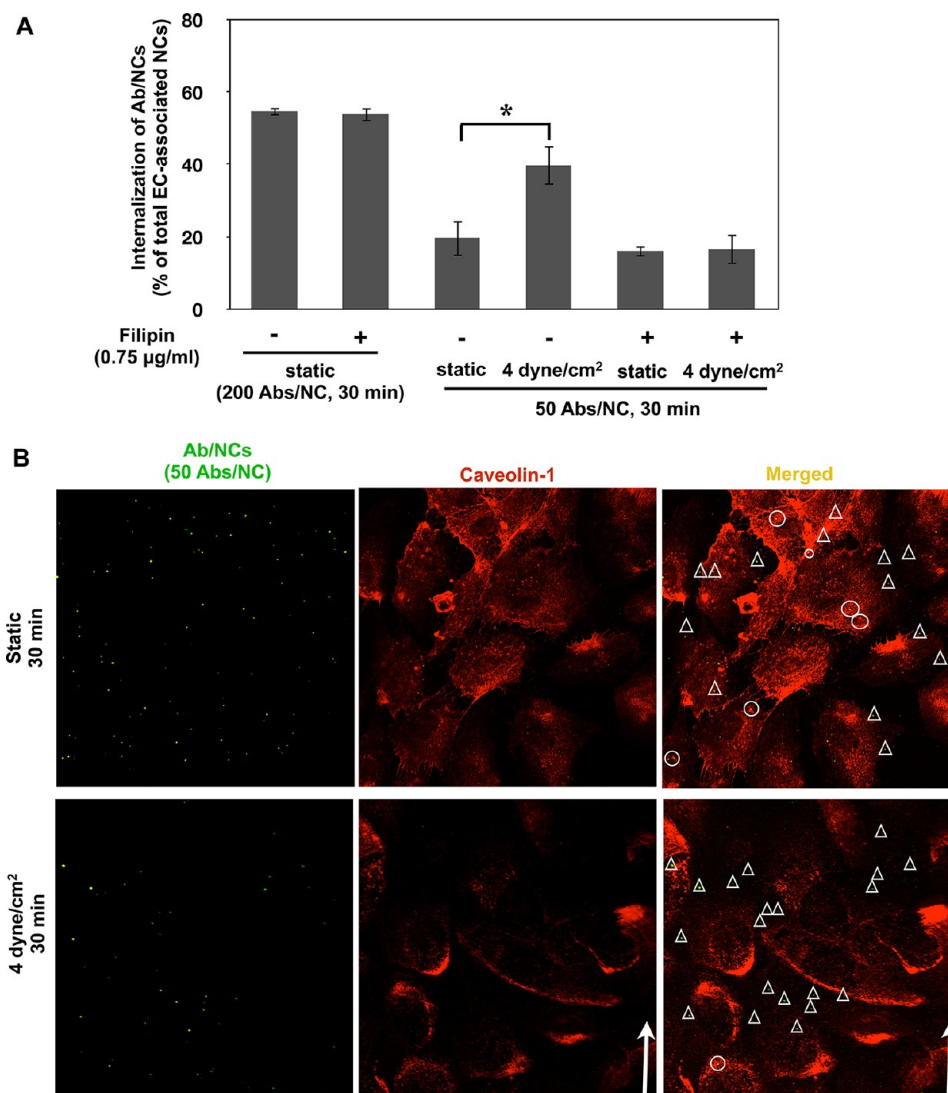


**Figure 6.** Cholesterol-rich membrane domains in endothelial cells are involved in stimulation of anti-PECAM/NC endocytosis by acute flow. (A) Disruption of cholesterol-enriched plasmalemma domains by filipin abolishes flow induced stimulation of endocytosis of low-avidity Ab/NC; mean  $\pm$  SE ( $n = 8$ ,  $*p < 0.05$ ). (B) Ab/NC are not colocalized with caveolin-1 in endothelial cells either under static and flow conditions. Confluent EC were incubated or perfused with Ab/NC for 30 min at 37 °C, fixed, and immunostained for caveolin-1. Arrows indicate the direction of flow. Ab/NC in circles or triangles are colocalized (yellow) or noncolocalized (green) with caveolin-1, respectively.

shear-induced signaling cascades.<sup>58,59</sup> Either of these mechanisms can contribute to the effect observed in Figure 6: caveolar endocytosis may provide an additional entry for Ab/NC, thereby supplementing CAM-endocytosis, whereas flow-induced signaling may modulate CAM-endocytosis. However, the majority of cell-bound Ab/NC did not colocalize with caveolae marker (caveolin-1) neither in static nor in flow-exposed EC, and perhaps even more importantly, exposure to flow had no effect on colocalization of anti-PECAM/NCs with caveolae (Figure 6B). Based on these data, we speculate that the inhibitory effect of filipin pertains to caveolar or other lipid-raft domain signaling that assists the CAM-mediated endocytosis rather than to direct caveolar endocytosis. Nevertheless, the complexity and insufficient understanding of the effects of

flow on mutual influences of caveolar *versus* CAM-endocytosis mechanisms do not permit providing a definitive conclusion at the present time. However, regardless of the specific role of caveolae in this effect (*i.e.*, indirect signaling vs direct endocytic), it is important to remember that concentration of caveoli varies greatly in different vessels, from abundance in pulmonary capillaries to lack in the cerebral arteries. It is quite plausible that differences in caveolar pathways in different vessels contribute to modulation of endocytosis anti-PECAM/NC, along with other factors including hydrodynamic characteristics. Dissection of these intricate inter-relationships is extremely intriguing and challenging, in part due to the fact that hydrodynamic factors regulate caveoli in endothelial cells.<sup>59</sup> Interestingly, genetic ablation of caveolin-1 has been reported



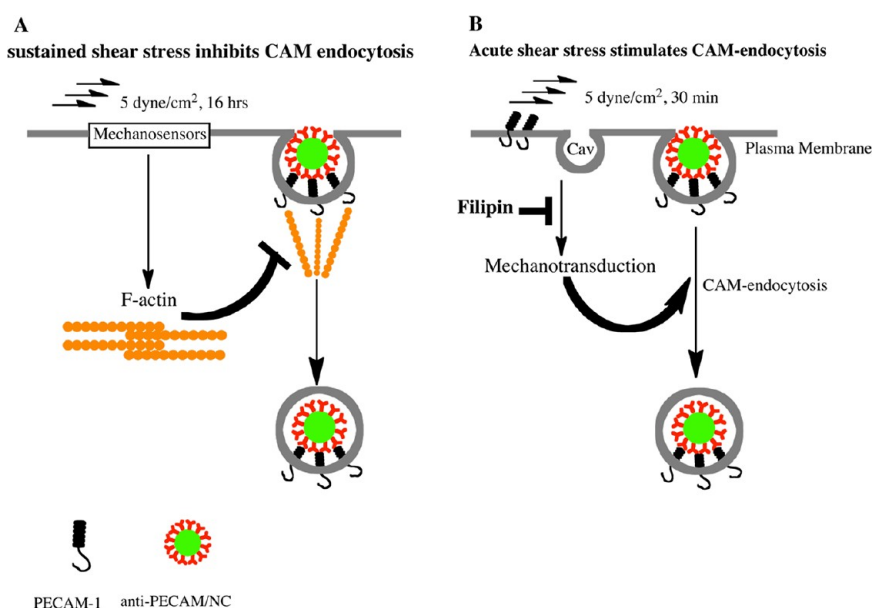


**Figure 7.** Chronic and acute flow differently regulate endocytosis of anti-PECAM/NC. (A) Sustained exposure of EC to flow induces formation of actin stress fibers involved in cellular alignment, which impairs recruitment of actin in the fibers needed for endocytosis of Ab/NC. (B) Acute exposure of EC to flow stimulates endocytosis of Ab/NC likely *via* mechanisms involving cholesterol-rich domains of plasmalemma such as caveoli (cav).

not to affect endocytosis of Ab/NCs targeted to ICAM expressed on pulmonary capillary endothelium *in vivo*.<sup>60</sup>

Noteworthy, a fraction of endothelial PECAM-1 has been found in subplasmalemmal vesicles undergoing dynamic cycles of fusion with and separation from the plasmalemma, thereby providing a pool of PECAM-1 that can be mobilized to the cell surface.<sup>61</sup> It is intriguing to speculate that the dynamic pool of PECAM-1 provided by this unusual and highly stochastic mechanism can play a role in flow-dependent mechanisms of anti-PECAM/NC uptake. Future studies of the kinetics and subcellular distribution of PECAM molecules involved in Ab/NC endocytosis under flow will help to clarify this interesting question.

ECs possess numerous mechanoreceptors responding to flow,<sup>24,37,62</sup> including PECAM itself.<sup>41</sup> Acute shear stress generates tension between adjacent endothelial cells and causes phosphorylation of PECAM cytoplasmic tail, initiating flow-mediated intracellular signaling pathways.<sup>52</sup> Additional mechanotransduction sites include focal adhesions and caveolae where a signaling network composed of  $\beta 1$  integrin and caveolin-1 develops in response to fluid shear stress.<sup>63,64</sup> Many (if not all) shear stress induced signals lead to actin remodeling.<sup>65</sup> The present results also imply relationships between flow, actin remodeling, and endocytosis of Ab/NC. As Figure 7 illustrates, endocytosis of anti-PECAM/NCs is inhibited by chronic flow, likely *via* actin restructuring limiting its ability to support endocytosis. In contrast, acute shear stress stimulates endocytosis of anti-PECAM/NCs, likely *via* signaling mediated by mechanosensing in cholesterol-rich domains of the plasmalemma.

**TABLE 1.** Characterization of Anti-PECAM/NC<sup>a</sup>

	$D_{avg}$ (nm)	polydispersity (PD)	zeta potential (mV)
uncoated NC	125 ± 4	0.05	-58.5
control (IgG) NC	187 ± 8	0.17	-0.6
50 Ab/NC	193 ± 9	0.18	-0.8
100 Ab/NC	194 ± 6	0.24	-1.3
200 Ab/NC	202 ± 9	0.24	0.1

<sup>a</sup> Average hydrodynamic radius,  $D_{avg}$ , PD, and zeta potential for a PECAM-NC were determined by DLS.

Therefore, acute and chronic shear stress, and other features of endothelial phenotype (e.g., thrombin activation), distinctly modulate endocytosis of PECAM-targeted nanocarriers. Some of these factors have opposing effects on Ab/NC binding *versus* endocytosis. These findings open a relatively underappreciated aspect of intracellular drug delivery and vascular transport. From the standpoint of endothelial targeting, this indicates that intracellular delivery will differ in distinct segments of the vasculature and that pathological factors may further modulate this process. Taken in the context with a recent finding of deceleration of endothelial endocytosis of anti-ICAM/NP by adaptation to chronic flow,<sup>50</sup> our results reinforce the translational significance of understanding of factors of cellular microenvironment in drug delivery. In theory, the effects of this modulation can be tuned by optimization of carrier design. For example, our results indicate that increase of the avidity of nanocarriers can both maximize the binding under flow and minimize the effects of flow on endocytosis. Carrier geometry (size and shape) is also known to influence targeting

and endocytosis.<sup>35,38</sup> This study is focused on the flow effect on endocytosis of spheres with ~200 nm diameter, and it is conceivable that endocytosis of carriers with distinct geometries will be differently regulated by flow.

Similar effects of flow on the endocytosis of anti-PECAM/NC and anti-ICAM/NC imply that there may be other endothelial transport processes similarly influenced by flow (e.g., uptake of nanocarriers targeted to other molecules, uptake of physiological circulating nanoparticles including lipoproteins, etc.). Our data suggest that the effect of chronic flow is mediated by reorganization of the cytoskeleton, a major regulator of diverse pathways for intracellular uptake and traffic.<sup>3,8,66</sup> More generally, the results alert us to the necessity of studying drug delivery in experimental models that adequately address the typical microenvironment

of the target cell including biochemical and biomechanical factors such as flow and ischemia for endothelial cells, contraction for muscle cells, and stretch for alveolar epithelial cells.<sup>67,68</sup>

## CONCLUSION

It is necessary to investigate intracellular delivery using models that include the contribution of (patho)physiological factors typical of the cell type and its microenvironment. This paper represents the first attempt to define the role of the hydrodynamic microenvironment in the uptake of Ab/NC targeted to endothelium *via* cell adhesion molecule PECAM(CD31). Most likely, flow-mediated modulation of Ab/NC endocytosis occurs in the vasculature and may differentially influence the delivery of Ab/NC in distinct vascular areas.

## METHODS

**Materials.** Monoclonal antibodies to human and mouse PECAM-1 (anti-PECAM) were Ab62, kindly provided by Dr. Marian Nakada (Centocor)<sup>18</sup> and MEC-13.3 (BD Biosciences, San Jose, CA), respectively. Mouse IgG was from Jackson Immuno-Research Laboratory, Inc. (West Grove, PA). Polyclonal antibody against human caveolin-1 was purchased from Cell Signaling Technology (Danvers, MA). Fluorescent secondary antibodies and phalloidin were from Invitrogen (Carlsbad, CA). Fluorescein isothiocyanate (FITC)-labeled polystyrene spheres (~125 nm in effective diameter) were purchased from Polysciences (Warrington, PA). Filipin was obtained from Sigma (St. Louis, MO).

**Preparation of Anti-PECAM/NCs.** FITC-labeled polystyrene spheres were coated with either anti-PECAM or control murine IgG using incubation at room temperature (RT) for 1 h,<sup>19</sup> centrifuged to remove unbound materials, then resuspended in 1% bovine serum albumin (BSA)-PBS and microsonicated for 20 s at low power. The effective immunobead diameter was determined by dynamic light scattering (DLS) using a BI-90 Plus particle size analyzer with BI-9000AT Digital autocorrelator (Brookhaven Instruments, Brookhaven, NY). This protocol yields uniform preparations of anti-PECAM/NC with particle diameters ranging from 180 to 200 nm, indicated thereafter as Ab/NC unless specified otherwise. The saturating antibody surface coverage on the NC surface was estimated to be ~200 antibody molecules per particle, which is referenced as 100% coverage.<sup>69</sup> To prepare Ab/NCs with variable antibody surface densities (50, 100, and 200 anti-PECAM molecules per NC), the polystyrene spheres were coated with a mix of anti-PECAM antibody and IgG at molar ratios 1:3, 1:1, and 1:0, respectively, keeping the total amount of IgG molecules coated per particle (including anti-PECAM and IgG) constant to avoid variability due to different surface coatings.<sup>69</sup> Characterizations of anti-PECAM/NCs are shown in Table 1. Prior studies have shown that antibody coated on the particle surface obtained by this protocol is stable: neither incubation with excessive amounts of BSA nor several rounds of harsh pipetting, sonication, or centrifugation and resuspension caused detachment of radiolabeled IgG molecules from the particles.<sup>14,43</sup>

**Immunofluorescence Microscopy of Lung Tissue Sections.** Animal experiments were performed according to the protocol approved by the Institutional Animal Care and Use Committee (IACUC) of the University of Pennsylvania. FITC-polystyrene nanoparticles coated with ~200 molecules of rat antibody against murine PECAM-1 were injected into C57BL/6J mice (Jackson Laboratory, Bar Harbor, ME) *via* the jugular vein. A total of 30 min after injection, the lungs were ventilated and

perfused *via* the pulmonary artery with ice-cold RPMI-1640 medium until all blood was completely washed out; the cold temperature arrested endocytosis. Medium containing 1% paraformaldehyde was perfused for 5 min to fix the pulmonary endothelium, followed by extensive washing with perfusion medium. The pulmonary vasculature was then perfused with a buffer containing Alexa Fluor 594 antibody to rat IgG for 15 min to counterstain endothelial surface bound Ab/NCs. After further washing to remove unbound secondary antibody, the lungs were filled with cold melting 1% agarose *via* the trachea and the vessels were perfused with 4% paraformaldehyde and 0.5% glutaraldehyde in 0.1 M sodium cacodylate buffer for 10 min. Lungs were then excised and kept in fixation solution for 4 h prior to cryosectioning. Fluorescence and transmission images were acquired using a laser scanning confocal microscope (Bio-Rad Radiance 2000).

***In Vitro* Laminar Shear Stress System.** A six-channel  $\mu$ -microslide (Ibidi, Germany) was used to subject HUVEC monolayers to defined laminar shear stress. The microslide was connected to a recirculating flow circuit composed of a variable-speed peristaltic pump (Rainin RP-1, Columbus, OH), a reservoir with culture medium, and inlet and outlet silicone rubber tubing. The flow rate was calibrated by collecting the volume of medium discharged per minute. The wall shear stress generated by fluid flow through the fully developed channel was calculated using  $\tau(\text{dyn/cm}^2) = 6\mu Q/H^3W$ , where  $\mu$  is the fluid viscosity ( $\mu = 0.70$  cP for HBSS at 37 °C),  $Q$  is the mean velocity of the flow through the channel, and  $H$  and  $W$  are the channel height (0.4 mm) and width (3.8 mm), respectively. Shear stresses were in the range 0–8 dyn/cm<sup>2</sup>. The temperature was maintained at 37 °C, and pH and gases were maintained in a 95% air/5% CO<sub>2</sub> incubation chamber.

**Cell Culture and Treatments.** Human umbilical vein endothelial cells (HUVECs) at passage 1 were purchased from Lonza (Walkersville, MD) and cultured for up to six passages in EGM-2 SingleQuotes supplemented with 10% fetal bovine serum (Lonza). HUVECs were starved overnight in endothelial basal medium (EBM) containing 0.5% fetal bovine serum without supplements prior to experiments. Anti-PECAM or IgG coated nanocarriers were then added to HBSS in the reservoir to the final carrier concentration of  $2.0 \times 10^9$  carriers/mL, unless specified otherwise, and were perfused or incubated for 30 min. Thereafter, cells were washed extensively with HBSS to remove unbound particles prior to fixation with 1% paraformaldehyde for fluorescent staining and analysis. Our goal was to compare the uptake at different conditions. Therefore, we wanted to avoid the saturation of the process and choose 30 min time point that is about half-time for saturation that reaches more than 80% internalization by approximately 60 min.<sup>19</sup>

In the experiments to examine the effect of filipin on endocytosis of Ab/NCs, HUVECs were preincubated with filipin (0.75  $\mu\text{g}/\text{mL}$ ) for 30 min. Thereafter, cells were incubated or perfused with anti-PECAM/NCs in the presence of filipin.

The human mesothelioma REN cells stably transfected with human wild-type PECAM-1 or cytoplasmic domain deleted mutant  $\Delta\text{PECAM-1}$ , used in this study, have been previously described.<sup>23</sup> REN cells were cultured in RPMI1640 medium supplemented with 10% FBS and geneticin (G418) as a selection agents.

**Microscopy and Quantification of Cell-Bound and Internalized Anti-CAM/NCs.** HUVEC monolayers or REN cells were washed with Hank's balanced salt solution (HBSS) to remove unbound nanocarriers following endothelial uptake of Ab/NCs. Cells were then fixed with 1% paraformaldehyde for 10 min. To distinguish between surface-bound or internalized immunobeads, nonpermeabilized fixed cells were counterstained for 30 min at RT with Alexa-Fluor-594-conjugated goat antimouse IgG to produce double-labeled, yellow particles. The cells were washed five times with HBSS containing 0.05% Tween-20, mounted with ProLong Antifade Kit (Molecular probes, Eugene OR), and analyzed by fluorescence microscopy.

HUVECs grown in the flow chamber were exposed to FSS (5  $\text{dyn}/\text{cm}^2$ ) for 16 h. Cells were fixed, permeabilized with 0.1% Triton X-100 for 15 min, and stained for F-actin (stress fibers) with Alexa-Fluor-594-phalloidin (Molecular probes, Eugene, OR).

For microscopy, samples were observed using an Olympus IX70 inverted fluorescence microscope, 40 $\times$  PlanApo objectives and filters optimized for green fluorescence (excitation BP460–490 nm, dichroic DM570 nm, emission BA515–550 nm) and red fluorescence (excitation BP530–550 nm, dichroic DM570 nm, emission BA590–800+). Separate images for each fluorescence channel were acquired using a Hamamatsu Orca-1 CCD camera. The images were merged and analyzed with ImagePro 3.0 imaging software (Media Cybernetics, Silver Spring, MD). For quantification, merged images of cells labeled with immunobeads are scored automatically for total green fluorescent particles and separately for noninternalized immunobeads (double-labeled yellow particles). Endocytosis was calculated as the percentage of internalized immunobeads with respect to the total number of cell-associated immunobeads. The data are shown as means from  $\geq 6$  images  $\pm$  SE. Statistical significance between groups was determined by student's *t* test and was accepted as significant at  $p < 0.05$ .

**Conflict of Interest:** The authors declare no competing financial interest.

**Acknowledgment.** This study is supported by R01 HL073940 and HL087036 (V.R.M) and support of NRSA through a fellowship in the Institute of Engineering and Medicine (P.F.D.) is gratefully acknowledged.

**Supporting Information Available:** Supplemental Figure 1. Anti-PECAM/NC is specifically targeted to pulmonary endothelium *in vivo*. Ab/NCs demonstrated markedly increased fluorescence compared to IgG/NC (30 min post-IV injection) in *naive* mice. Arrows in lower panels indicate the minimal amount of fluorescence due to nonspecific pulmonary accumulation of untargeted particles. This material is available free of charge via the Internet at <http://pubs.acs.org>.

## REFERENCES AND NOTES

1. Champion, J. A.; Mitragotri, S. Role of Target Geometry in Phagocytosis. *Proc. Natl. Acad. Sci. U.S.A.* **2006**, *103*, 4930–4934.
2. Gratton, S. E.; Ropp, P. A.; Pohlhaus, P. D.; Luft, J. C.; Madden, V. J.; Napier, M. E.; DeSimone, J. M. The Effect of Particle Design on Cellular Internalization Pathways. *Proc. Natl. Acad. Sci. U.S.A.* **2008**, *105*, 11613–11618.
3. Reilly, M. J.; Larsen, J. D.; Sullivan, M. O. Polyplexes Traffic through Caveolae to the Golgi and Endoplasmic Reticulum en Route to the Nucleus. *Mol. Pharm.* **2012**, *9*, 1280–1290.
4. Bonner, D. K.; Leung, C.; Chen-Liang, J.; Chingozha, L.; Langer, R.; Hammond, P. T. Intracellular Trafficking of Polyamidoamine-Poly(ethylene glycol) Block Copolymers

in DNA Delivery. *Bioconjugate Chem.* **2011**, *22*, 1519–1525.

5. Evans, C. W.; Fitzgerald, M.; Clemons, T. D.; House, M. J.; Padman, B. S.; Shaw, J. A.; Saunders, M.; Harvey, A. R.; Zdyrko, B.; Luzinov, I.; et al. Multimodal Analysis of PEI-Mediated Endocytosis of Nanoparticles in Neural Cells. *ACS Nano* **2011**, *5*, 8640–8648.
6. Holt, B. D.; Dahl, K. N.; Islam, M. F. Cells Take up and Recover from Protein-Stabilized Single-Wall Carbon Nanotubes with Two Distinct Rates. *ACS Nano* **2012**, *6*, 3481–3490.
7. Oh, E.; Delehanty, J. B.; Sapsford, K. E.; Susumu, K.; Goswami, R.; Blanco-Canosa, J. B.; Dawson, P. E.; Granek, J.; Shoff, M.; Zhang, Q.; et al. Cellular Uptake and Fate of PEGylated Gold Nanoparticles is Dependent on Both Cell-Penetration Peptides and Particle Size. *ACS Nano* **2011**, *5*, 6434–6448.
8. Iversen, T.-G.; Skotland, T.; Sandvig, K. Endocytosis and Intracellular Transport of Nanoparticles: Present Knowledge and Need for Future Studies. *Nano Today* **2011**, *6*, 176–185.
9. Ding, B. S.; Dziubla, T.; Shuvaev, V. V.; Muro, S.; Muzykantov, V. R. Advanced Drug Delivery Systems that Target the Vascular Endothelium. *Mol. Interventions* **2006**, *6*, 98–112.
10. Simone, E.; Ding, B. S.; Muzykantov, V. Targeted Delivery of Therapeutics to Endothelium. *Cell Tissue Res.* **2009**, *335*, 283–300.
11. Scherpereel, A.; Rome, J. J.; Wiewrodt, R.; Watkins, S. C.; Harshaw, D. W.; Alder, S.; Christofidou-Solomidou, M.; Haut, E.; Murciano, J. C.; Nakada, M.; et al. Platelet-Endothelial Cell Adhesion Molecule-1-Directed Immunotargeting to Cardiopulmonary Vasculature. *J. Pharmacol. Exp. Ther.* **2002**, *300*, 777–786.
12. Ding, B. S.; Hong, N.; Murciano, J. C.; Ganguly, K.; Gottstein, C.; Christofidou-Solomidou, M.; Albelda, S. M.; Fisher, A. B.; Cines, D. B.; Muzykantov, V. R. Prophylactic Thrombolysis by Thrombin-Activated Latent Prourokinase Targeted to PECAM-1 in the Pulmonary Vasculature. *Blood* **2008**, *111*, 1999–2006.
13. Dziubla, T. D.; Shuvaev, V. V.; Hong, N. K.; Hawkins, B. J.; Madesh, M.; Takano, H.; Simone, E.; Nakada, M. T.; Fisher, A.; Albelda, S. M.; et al. Endothelial Targeting of Semi-Permeable Polymer Nanocarriers for Enzyme Therapies. *Biomaterials* **2008**, *29*, 215–227.
14. Hsu, J.; Northrup, L.; Bhowmick, T.; Muro, S. Enhanced Delivery of Alpha-Glucosidase for Pompe Disease by ICAM-1-Targeted Nanocarriers: Comparative Performance of a Strategy for Three Distinct Lysosomal Storage Disorders. *Nanomedicine* **2011**, *8*, 731–739.
15. Xiao, Z.; Levy-Nissenbaum, E.; Alexis, F.; Luptak, A.; Tply, B. A.; Chan, J. M.; Shi, J.; Digga, E.; Cheng, J.; Langer, R.; et al. Engineering of Targeted Nanoparticles for Cancer Therapy Using Internalizing Aptamers Isolated by Cell-Uptake Selection. *ACS Nano* **2012**, *6*, 696–704.
16. McIntosh, D. P.; Tan, X. Y.; Oh, P.; Schnitzer, J. E. Targeting Endothelium and Its Dynamic Caveolae for Tissue-Specific Transcytosis *In Vivo*: a Pathway to Overcome Cell Barriers to Drug and Gene Delivery. *Proc. Natl. Acad. Sci. U.S.A.* **2002**, *99*, 1996–2001.
17. Medina-Kauwe, L. K. "Alternative" Endocytic Mechanisms Exploited by Pathogens: New Avenues for Therapeutic Delivery? *Adv. Drug Delivery Rev.* **2007**, *59*, 798–809.
18. Muzykantov, V. R.; Christofidou-Solomidou, M.; Balyashnikova, I.; Harshaw, D. W.; Schultz, L.; Fisher, A. B.; Albelda, S. M. Streptavidin Facilitates Internalization and Pulmonary Targeting of an Anti-Endothelial Cell Antibody (Platelet-Endothelial Cell Adhesion Molecule 1): a Strategy for Vascular Immunotargeting of Drugs. *Proc. Natl. Acad. Sci. U.S.A.* **1999**, *96*, 2379–2384.
19. Muro, S.; Wiewrodt, R.; Thomas, A.; Koniari, L.; Albelda, S. M.; Muzykantov, V. R.; Koval, M. A Novel Endocytic Pathway Induced by Clustering Endothelial ICAM-1 or PECAM-1. *J. Cell Sci.* **2003**, *116*, 1599–1609.
20. Muro, S. New Biotechnological and Nanomedicine Strategies for Treatment of Lysosomal Storage Disorders. *Wiley Interdiscip. Rev. Nanomed. Nanobiotechnol.* **2010**, *2*, 189–204.

21. Shuvaev, V. V.; Han, J.; Yu, K. J.; Huang, S.; Hawkins, B. J.; Madesh, M.; Nakada, M.; Muzykantov, V. R. PECAM-Targeted Delivery of SOD Inhibits Endothelial Inflammatory Response. *FASEB J.* **2011**, *25*, 348–357.
22. Han, J.; Shuvaev, V. V.; Muzykantov, V. R. Catalase and Superoxide Dismutase Conjugated with Platelet-Endothelial Cell Adhesion Molecule Antibody Distinctly Alleviate Abnormal Endothelial Permeability Caused by Exogenous Reactive Oxygen Species and Vascular Endothelial Growth Factor. *J. Pharmacol. Exp. Ther.* **2011**, *338*, 82–91.
23. Garnacho, C.; Shuvaev, V.; Thomas, A.; McKenna, L.; Sun, J.; Koval, M.; Albelda, S.; Muzykantov, V.; Muro, S. RhoA Activation and Actin Reorganization Involved in Endothelial CAM-Mediated Endocytosis of Anti-PECAM Carriers: Critical Role for Tyrosine 686 in the Cytoplasmic Tail of PECAM-1. *Blood* **2008**, *111*, 3024–3033.
24. Davies, P. F. Hemodynamic Shear Stress and the Endothelium in Cardiovascular Pathophysiology. *Nat. Clin. Pract. Cardiovasc. Med.* **2009**, *6*, 16–26.
25. Ando, J.; Yamamoto, K. Vascular Mechanobiology: Endothelial Cell Responses to Fluid Shear Stress. *Circ. J.* **2009**, *73*, 1983–1992.
26. Helmke, B. P. Molecular Control of Cytoskeletal Mechanics by Hemodynamic Forces. *Physiology* **2005**, *20*, 43–53.
27. Eniola, A. O.; Krasik, E. F.; Smith, L. A.; Song, G.; Hammer, D. A. I-Domain of Lymphocyte Function-Associated Antigen-1 Mediates Rolling of Polystyrene Particles on ICAM-1 under Flow. *Biophys. J.* **2005**, *89*, 3577–3588.
28. Charoenphol, P.; Huang, R. B.; Eniola-Adefeso, O. Potential Role of Size and Hemodynamics in the Efficacy of Vascular-Targeted Spherical Drug Carriers. *Biomaterials* **2010**, *31*, 1392–1402.
29. Ham, A. S.; Goetz, D. J.; Klibanov, A. L.; Lawrence, M. B. Microparticle Adhesive Dynamics and Rolling Mediated by Selectin-Specific Antibodies under Flow. *Biotechnol. Bioeng.* **2007**, *96*, 596–607.
30. Davies, P. F.; Dewey, C. F., Jr; Bussolari, S. R.; Gordon, E. J.; Gimbrone, M. A., Jr Influence of Hemodynamic Forces on Vascular Endothelial Function. *In Vitro Studies of Shear Stress and Pinocytosis in Bovine Aortic Cells. J. Clin. Invest.* **1984**, *73*, 1121–1129.
31. Sprague, E. A.; Steinbach, B. L.; Nerem, R. M.; Schwartz, C. J. Influence of a Laminar Steady-State Fluid-Imposed Wall Shear Stress on the Binding, Internalization, and Degradation of Low-Density Lipoproteins by Cultured Arterial Endothelium. *Circulation* **1987**, *76*, 648–656.
32. Traore, M.; Sun, R. J.; Fawzi-Grancher, S.; Dumas, D.; Qing, X.; Santus, R.; Stoltz, J. F.; Muller, S. Kinetics of the Endocytotic Pathway of Low Density Lipoprotein (LDL) in Human Endothelial Cells Line under Shear Stress: an *In Vitro* Confocal Microscopy Study. *Clin. Hemorheol. Microcirc.* **2005**, *33*, 243–251.
33. Niwa, K.; Sakai, J.; Karino, T.; Aonuma, H.; Watanabe, T.; Ohyama, T.; Inanami, O.; Kuwabara, M. Reactive Oxygen Species Mediate Shear Stress-Induced Fluid-Phase Endocytosis in Vascular Endothelial Cells. *Free Radical Res.* **2006**, *40*, 167–174.
34. Simone, E. A.; Dziubla, T. D.; Muzykantov, V. R. Polymeric Carriers: Role of Geometry in Drug Delivery. *Expert Opin. Drug Delivery* **2008**, *5*, 1283–1300.
35. Decuzzi, P.; Pasqualini, R.; Arap, W.; Ferrari, M. Intravascular Delivery of Particulate Systems: Does Geometry Really Matter? *Pharm. Res.* **2009**, *26*, 235–243.
36. Lin, A.; Sabnis, A.; Kona, S.; Nattama, S.; Patel, H.; Dong, J. F.; Nguyen, K. T. Shear-Regulated Uptake of Nanoparticles by Endothelial Cells and Development of Endothelial-Targeting Nanoparticles. *J. Biomed. Mater. Res., Part A* **2010**, *93*, 833–842.
37. Davies, P. F.; Spaan, J. A.; Krams, R. Shear Stress Biology of the Endothelium. *Ann. Biomed. Eng.* **2005**, *33*, 1714–1718.
38. Muro, S.; Garnacho, C.; Champion, J. A.; Leferovich, J.; Gajewski, C.; Schuchman, E. H.; Mitragotri, S.; Muzykantov, V. R. Control of Endothelial Targeting and Intracellular Delivery of Therapeutic Enzymes by Modulating the Size and Shape of ICAM-1-Targeted Carriers. *Mol. Ther.* **2008**, *16*, 1450–1458.
39. Liu, J.; Weller, G. E.; Zern, B.; Ayyaswamy, P. S.; Eckmann, D. M.; Muzykantov, V. R.; Radhakrishnan, R. Computational Model for Nanocarrier Binding to Endothelium Validated Using *In Vivo*, *In Vitro*, and Atomic Force Microscopy Experiments. *Proc. Natl. Acad. Sci. U.S.A.* **2010**, *107*, 16530–16535.
40. Calderon, A. J.; Bhowmick, T.; Leferovich, J.; Burman, B.; Pichette, B.; Muzykantov, V.; Eckmann, D. M.; Muro, S. Optimizing Endothelial Targeting by Modulating the Antibody Density and Particle Concentration of Anti-ICAM Coated Carriers. *J. Controlled Release* **2011**, *150*, 37–44.
41. Fujiwara, K. Platelet Endothelial Cell Adhesion Molecule-1 and Mechanotransduction in Vascular Endothelial Cells. *J. Intern. Med.* **2006**, *259*, 373–380.
42. Shuvaev, V. V.; Ilies, M. A.; Simone, E.; Zaitsev, S.; Kim, Y.; Cai, S.; Mahmud, A.; Dziubla, T.; Muro, S.; Discher, D. E.; et al. Endothelial Targeting of Antibody-Decorated Polymeric Filomicelles. *ACS Nano* **2011**, *5*, 6991–6999.
43. Simone, E. A.; Zern, B. J.; Chacko, A. M.; Mikitsh, J. L.; Blankemeyer, E. R.; Muro, S.; Stan, R. V.; Muzykantov, V. R. Endothelial Targeting of Polymeric Nanoparticles Stably Labeled with the PET Imaging Radioisotope Iodine-124. *Biomaterials* **2012**, *33*, 5406–5413.
44. Yue, T.; Zhang, X. Cooperative Effect in Receptor-Mediated Endocytosis of Multiple Nanoparticles. *ACS Nano* **2012**, *6*, 3196–3205.
45. Calderon, A. J.; Muzykantov, V.; Muro, S.; Eckmann, D. M. Flow Dynamics, Binding, and Detachment of Spherical Carriers Targeted to ICAM-1 on Endothelial Cells. *Biorheology* **2009**, *46*, 323–341.
46. Fung, Y. C. Stochastic Flow in Capillary Blood Vessels. *Microvasc. Res.* **1973**, *5*, 34–48.
47. Aird, W. C. Phenotypic Heterogeneity of the Endothelium: II. Representative Vascular Beds. *Circ. Res.* **2007**, *100*, 174–190.
48. Zhang, J. J.; Kelm, R. J.; Biswas, P.; Kashgarian, M.; Madri, J. A. PECAM-1 Modulates Thrombin-Induced Tissue Factor Expression on Endothelial Cells. *J. Cell. Physiol.* **2007**, *210*, 527–537.
49. Privratsky, J. R.; Paddock, C. M.; Florey, O.; Newman, D. K.; Muller, W. A.; Newman, P. J. Relative Contribution of PECAM-1 Adhesion and Signaling to the Maintenance of Vascular Integrity. *J. Cell Sci.* **2011**, *124*, 1477–1485.
50. Bhowmick, T.; Berk, E.; Cui, X.; Muzykantov, V. R.; Muro, S. Effect of Flow on Endothelial Endocytosis of Nanocarriers Targeted to ICAM-1. *J. Controlled Release* **2011**, *157*, 485–492.
51. Hubbard, A. K.; Rothlein, R. InterCellular Adhesion Molecule-1 (ICAM-1) Expression and Cell Signaling Cascades. *Free Radical Biol. Med.* **2000**, *28*, 1379–1386.
52. Fujiwara, K.; Masuda, M.; Osawa, M.; Kano, Y.; Katoh, K. Is PECAM-1 a Mechanoresponsive Molecule? *Cell Struct. Funct.* **2001**, *26*, 11–17.
53. Yamamoto, K.; Korenaga, R.; Kamiya, A.; Ando, J. Fluid Shear Stress Activates Ca(2+) Influx into Human Endothelial Cells via P2 × 4 Purinoceptors. *Circ. Res.* **2000**, *87*, 385–391.
54. Wei, Z.; Costa, K.; Al-Mehdi, A. B.; Dodia, C.; Muzykantov, V.; Fisher, A. B. Simulated Ischemia in Flow-Adapted Endothelial Cells Leads to Generation of Reactive Oxygen Species and Cell Signaling. *Circ. Res.* **1999**, *85*, 682–689.
55. Zebda, N.; Dubrovskyi, O.; Birukov, K. G. Focal Adhesion Kinase Regulation of Mechanotransduction and Its Impact on Endothelial Cell Functions. *Microvasc. Res.* **2012**, *83*, 71–81.
56. Wang, Z.; Tiruppathi, C.; Cho, J.; Minshall, R. D.; Malik, A. B. Delivery of Nanoparticle: Crossed Drugs Across the Vascular Endothelial Barrier via Caveolae. *IUBMB Life* **2011**, *63*, 659–667.
57. Sverdlov, M.; Shajahan, A. N.; Minshall, R. D. Tyrosine Phosphorylation-Dependence of Caveolae-Mediated Endocytosis. *J. Cell. Mol. Med.* **2007**, *11*, 1239–1250.
58. Parton, R. G.; Simons, K. The Multiple Faces of Caveolae. *Nat. Rev. Mol. Cell Biol.* **2007**, *8*, 185–194.
59. Rizzo, V.; Morton, C.; DePaola, N.; Schnitzer, J. E.; Davies, P. F. Recruitment of Endothelial Caveolae into Mechanotransduction Pathways by Flow Conditioning *In Vitro*. *Am. J. Physiol. Heart Circ. Physiol.* **2003**, *285*, H1720–9.

60. Serrano, D.; Bhowmick, T.; Chadha, R.; Garnacho, C.; Muro, S. Intercellular Adhesion Molecule 1 Engagement Modulates Sphingomyelinase and Ceramide, Supporting Uptake of Drug Carriers by the Vascular Endothelium. *Arterioscler., Thromb., Vasc. Biol.* **2012**, *32*, 1178–1185.
61. Mamdouh, Z.; Chen, X.; Pierini, L. M.; Maxfield, F. R.; Muller, W. A. Targeted Recycling of PECAM from Endothelial Surface-Connected Compartments During Diapedesis. *Nature* **2003**, *421*, 748–753.
62. Lehoux, S.; Tedgui, A. Shear and Signal Transduction in the Endothelial Cell. *Med. Sci. (Paris)* **2004**, *20*, 551–556.
63. Ferraro, J. T.; Daneshmand, M.; Bizios, R.; Rizzo, V. Depletion of Plasma Membrane Cholesterol Dampens Hydrostatic Pressure and Shear Stress-Induced Mechanotransduction Pathways in Osteoblast Cultures. *Am. J. Physiol. Cell. Physiol* **2004**, *286*, C831–9.
64. Radel, C.; Carlile-Klusacek, M.; Rizzo, V. Participation of Caveolae in  $\beta$ 1 Integrin-Mediated Mechanotransduction. *Biochem. Biophys. Res. Commun.* **2007**, *358*, 626–631.
65. Yang, B.; Radel, C.; Hughes, D.; Kelemen, S.; Rizzo, V. p190Rho GTPase-Activating Protein Links the  $\beta$ 1 Integrin/Caveolin-1 Mechanosignaling Complex to RhoA and Actin Remodeling. *Arterioscler. Thromb. Vasc. Biol.* **2010**, *31*, 376–383.
66. Badding, M. A.; Vaughan, E. E.; Dean, D. A. Transcription Factor Plasmid Binding Modulates Microtubule Interactions and Intracellular Trafficking During Gene Transfer. *Gene Ther.* **2012**, *19*, 354.
67. Lam, A. P.; Dean, D. A. Cyclic Stretch-Induced Nuclear Localization of Transcription Factors Results in Increased Nuclear Targeting of Plasmids in Alveolar Epithelial Cells. *J. Gene Med.* **2008**, *10*, 668–678.
68. Eldib, M.; Dean, D. A. Cyclic Stretch of Alveolar Epithelial Cells Alters Cytoskeletal Micromechanics. *Biotechnol. Bioeng.* **2011**, *108*, 446–453.
69. Muro, S.; Dziubla, T.; Qiu, W.; Leferovich, J.; Cui, X.; Berk, E.; Muzykantov, V. R. Endothelial Targeting of High-Affinity Multivalent Polymer Nanocarriers Directed to Intercellular Adhesion Molecule 1. *J. Pharmacol. Exp. Ther.* **2006**, *317*, 1161–1169.